Single and twin string cavitation swirling flows in multi-hole mini-sac diesel injector and sprays

Nurcholik, Samsu Dlukha ; Sou, Akira ; Miwa, Takashi ; Kawaguchi, Mikimasa ; Matsumoto, Yuhei ; Nishida, Keiya ; Wada, Yoshitaka ; Ueki,…

(Citation)
Journal of Fluid Science and Technology,18(2):JFST0023

(Issue Date)
2023

(Resource Type)
journal article

(Version)
Version of Record

(URL)
https://hdl.handle.net/20.500.14094/0100482067

Bulletin of the JSME Vol.18, No.2, 2023
Journal of Fluid Science and Technology

Single and twin string cavitation swirling flows in multi-hole mini-sac diesel injector and sprays

Samsu Dlukha NURCHOLIK*,**, Akira SOU*, Takashi MIWA*, Mikimasa KAWAGUCHI***, Yuhei MATSUMOTO***, Keiya NISHIDA***, Yoshitaka WADA**** and Yoshiharu UEKI****

*Graduate School of Maritime Sciences, Kobe University,
5-1-1 Fukaeminami-machi, Higashinada-ku, Kobe 658-0012, Japan
E-mail: sou@maritime.kobe-u.ac.jp
**Department of Naval Architecture, Institut Teknologi Kalimantan,
Jalan Soekarno Hatta KM 15, Balikpapan 76127, Indonesia
***Graduate School of Advanced Science and Engineering, Hiroshima University,
1-4-1 Kagamiyama, Higashi-Hiroshima, Hiroshima 739-8527, Japan
****Engineering Analysis Group. No. 1, Mazda Motor Corporation
3-1 Shinchi, Fuchu-cho, Aki-gun, Hiroshima 730-8670, Japan

Received: 29 November 2022; Revised: 9 January 2023; Accepted: 26 January 2023

Abstract

A new design of fuel injector for diesel engines is expected to enhance fuel spray atomization at the end of the fuel injection for the reduction in particulate matter emission. It was pointed out that string cavitation may occur in a multi-hole mini-sac injector and increase spray angle. However, the complicated velocity distributions in the injectors have not been understood yet, which make it difficult for us to reveal the overall string cavitation phenomena. In this study, visualization of string cavitation in a transparent three-hole mini-sac injector and spray at various needle seat gaps and particle image velocimetry (PIV) analysis of the flow in a plane perpendicular to the axis of an orifice are carried out to clarify the cavitation and flow structure as well as spray characteristics. The results clarify that (1) at the low needle lift of $Z/D = 1$ twin string cavitation flow appears intermittently and (2) at the very low needle lift of $Z/D = 0.5$ single string cavitation flow with a hollow-cone spray occurs, which significantly increases spray angle.

Keywords : Diesel fuel injector, String cavitation, Spray angle, Particle image velocimetry, Circulation

1. Introduction

A large effort has been made to reduce the emissions of CO_2, NO_X and particulate matter (PM) from diesel engines. One of the most critical issues which contribute to the CO_2 and PM reductions is internal cavitating flow in the fuel injector (Schmidt and Corradini, 2001). A lot of researchers have been revealing the cavitation flow phenomenon (Bergwerk, 1959; Hiroyasu et al., 1991; Soteriou et al., 1995; Sou et al., 2007; Sou et al., 2008a, 2008b; Duke et al., 2017). It was clarified that super cavitation in a nozzle induces a large and strong turbulence, and enhances liquid jet atomization. Recently, it was pointed out that string cavitation may appear in multi-hole fuel injectors at low needle lift (Miranda et al., 2002; He et al., 2016; Wei et al., 2022), which increases spray angle (Hayashi et al., 2013; Pratama et al., 2016; Prasetya et al., 2021; Guan et al., 2021) and decreases droplet diameters (Mitroglou et al., 2011). Particle image velocimetry (PIV) analysis on a plane through the central axis of a sac of mini-sac injector was carried out to show the vortex flow in a sac (Hayashi et al., 2013; Prasetya et al., 2021). However, the previous researchers have used their own injectors with different geometries, and various patterns of the complicated three-dimensional velocity distributions in the injectors have not been clarified yet, which make it difficult for us to reveal the overall string cavitation flow phenomena.

In this study, we carry out visualization of string cavitation in a transparent three-hole mini-sac injector and sprays at different needle seat gaps as well as (PIV) analysis of the flow on a plane not through the central axis but perpendicular to the axis of an orifice to investigate string cavitation flows in the fuel injector.

Paper No.22-00453
[DOI: 10.1299/jfst.2023jfst0023]

2. Nomenclature

C_c	Contraction coefficient [-]
D	Diameter of the orifice [mm]
D_S	Diameter of the sac [mm]
L	Length of the orifice [mm]
ℓ	Distance between the orifice inlet and laser sheet [mm]
P	Injection pressure [MPa]
P_b	Back pressure [Pa]
P_v	Vapor saturation pressure [Pa]
P_{SC}	Probability of string cavitation appearance [-]
Re	Reynolds number [-]
S_O	Total cross-sectional area of orifices [mm^2]
S_S	Total cross-sectional area of seat [mm^2]
T	Temperature [K]
U	Measured local velocity by PIV analysis [m/s]
V	Mean velocity in an orifice [m/s]
Z	Needle seat gap [mm]
Γ	Circulation [m^2/s]
θ	Spray angle [degree]
θ_{Ne}	Needle tip angle [degree]
λ	Friction coefficient [-]
ρ	Liquid density [kg/m^3]
σ	Surface tension [N/m]
σ_c	Modified cavitation number [-]
ν	Liquid kinematic viscosity [m^2/s]
ω	vorticity [1/s]

3. Experimental setup

The experimental setup for high-speed imaging is shown in Fig. 1. Diesel fuel mixed with 21.0% of α-methylnaphthalene at 304 K in temperature was used to match the refractive index of the liquid with that of the acrylic, by which cavitation in the injector can be clearly observed and PIV analysis in the sac can be carried out. Liquid was injected from a pressure vessel constantly through the transparent acrylic three-hole mini-sac injector into the ambient air at room temperature. Liquid flowrate was measured by a flowmeter (Keyence FD-SS20A). A high-speed camera (Photron, FASTCAM SA-Z, 3500-5000 fps, exposure time = 10 μs, 40 μm/pixel) and a metal halide light (KYOWA co., ltd., MID-25FC, 250 W) were used for high-speed imaging. The details of the experimental setup were described in our previous paper (Prasetya et al., 2021).

The schematics of the injector is shown in Fig. 2. An enlarged three-hole mini-sac injector and a needle valve with a sharp needle tip whose tip angle θ_{Ne} was 60° was used. The sac diameter D_S, orifice length L, and orifice diameter D are 10.0, 8.0 and 2.0 mm, respectively. The transparent injector is about twenty times as large as the real diesel injectors. The experiments were conducted at the needle seat gaps of 1.0 and 2.0 mm (Z/D = 0.5 and 1). Experimental conditions are shown in Table 1, where the modified cavitation number σ_c (Hiroyasu et al., 1991; Sou et al., 2008a) is defined as

$$\sigma_c = {C_c}^2 \left[\frac{P_b - P_v}{\frac{1}{2}\rho V^2} + \frac{\lambda L}{D} + 1 \right] \tag{1}$$

where P_b represents the atmospheric pressure, P_v represents the saturation pressure, ρ represents the liquid density and λ represents the friction factor. The C_c is the contraction coefficient, and is 0.65. The Reynolds number Re is defined as

[DOI: 10.1299/jfst.2023jfst0023]

$$Re = \frac{VD}{\nu} \tag{2}$$

where ν is kinematic viscosity. We can clearly find that the effects of the refractive index matching on the diesel fuel property are negligible. The total cross-sectional areas of the orifices and seat are shown in Table 2. At Z/D = 1 and 0.5, the total cross-sectional area of the orifices S_O is smaller than that of seat S_S, which shows that the velocity at the orifice is larger than that at the seat.

Image processing was carried out to quantify the spray angle θ. The details on the image processing was described in our previous paper (Prasetya et al., 2021). The definitions of θ is illustrated in Fig. 3. Spray angle θ was measured at the distance of 2L from the orifice exit.

Figure 4(a) shows the experimental setup for PIV analysis, which consists of a high-speed camera (Photron, FASTCAM SA-Z, 20000 fps, exposure time = 10 μs, 1024 x 1024 pixels, 12 μm/pixels) and a green laser sheet generator (sheet light thickness = 1 mm). The fluorescent particles (FLUOSTAR, model 0459, 15 μm in mean diameter) were used as tracer particles. A commercial PIV software (FtrPIV, ver. 3.2.3.2, Flowtech Research Inc.) was used for PIV analysis. As illustrated in Fig. 4(b), green laser sheet was applied perpendicular to an orifice axis, and the distance ℓ between the orifice inlet and the laser sheet was set to 2 or 3 mm. The internal between the pair of the images was 10 μs, and the captured area was about 12 mm x 12 mm, by which the entire sac was covered. The interrogation window size was 16 x 16 pixels with 50% overlap, and the search window size was 33 x 33 pixels. Circulation in the region of 6 mm x 3 mm for single vortex flow and 3 mm x 3 mm for twin vortex flow around the orifice was calculated based on the PIV result, which is formulated by

$$\Gamma = \oint_C U \cdot dL \tag{3}$$

where U represents the velocity, and dL represents the line segment along the measurement region.

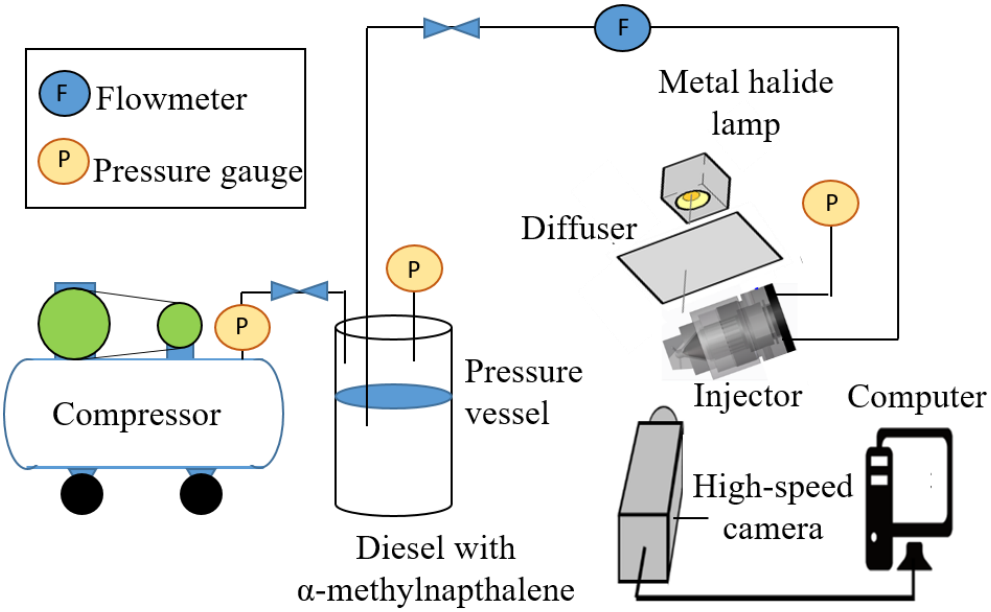

Fig. 1 Experimental setup for high-speed imaging

[DOI: 10.1299/jfst.2023jfst0023]

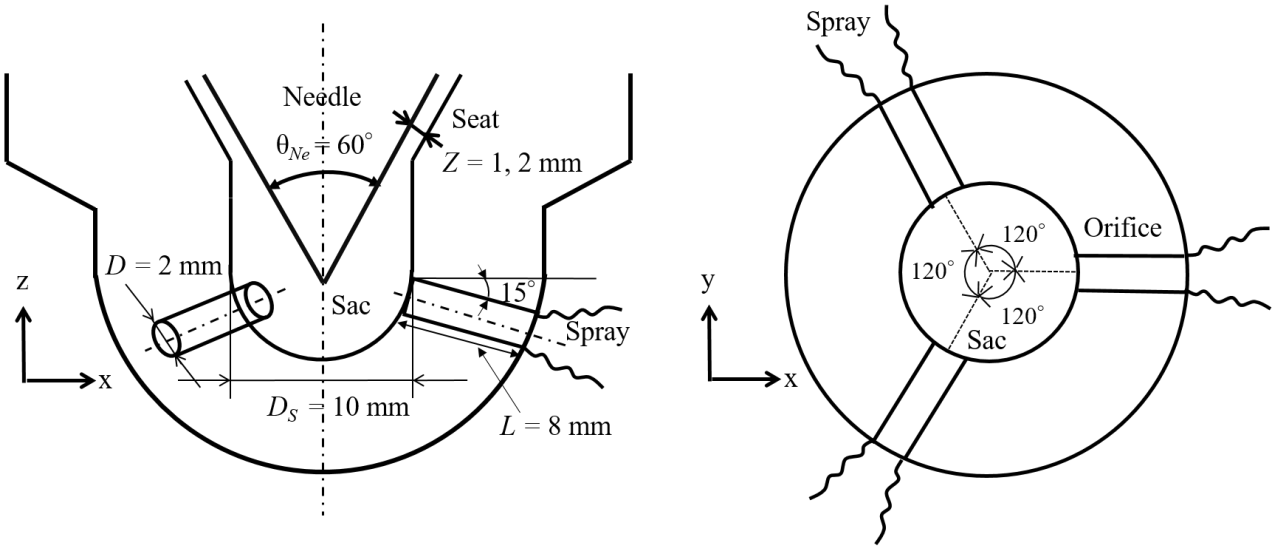

(a) Front view (b) Bottom view

Fig. 2 Schematic of three-hole mini-sac injector

Table 1 Experimental condition

Item	This study	Real injection
Orifice diameter D [mm]	2.0	0.1
Needle seat gap Z [mm]	2.0, 1.0 (Z/D = 1, 0.5)	0.01 - 0.05 (Z/D = 1, 0.5)
Orifice length L [mm]	8.0 (L/D = 4)	0.4 (L/D = 4)
Sac diameter D_S [mm]	10.0	0.5
Mean velocity at orifice V [m/s]	3 - 16	10 - 80
Injection pressure P [MPa]	0.08 - 0.25	200 - 300
Liquid temperature T [K]	304 ± 2	-
Liquid	Diesel with α-methylnaphthalene	Diesel
Liquid density ρ [kg/m^3]	865	780 - 900
Surface tension σ [N/m]	0.027	0.021 - 0.028
Liquid kinematic viscosity ν [m^2/s]	3.3 x 10^{-6}	2.0 x 10^{-6} – 3.5 x 10^{-6}
Modified cavitation number σ_c [-]	0.76 - 5.0	0.75 - 2.5
Reynolds number [-]	0 - 20000	0 - 7000

Table 2 Total cross-sectional areas of orifices and seat

Needle seat gap Z [mm]	Z/D [-]	Total cross-sectional area of orifices S_O [mm^2]	Total cross-sectional area of seat S_S [mm^2]
2.0	1	9.42	52.32
1.0	0.5	9.42	28.98

[DOI: 10.1299/jfst.2023jfst0023]

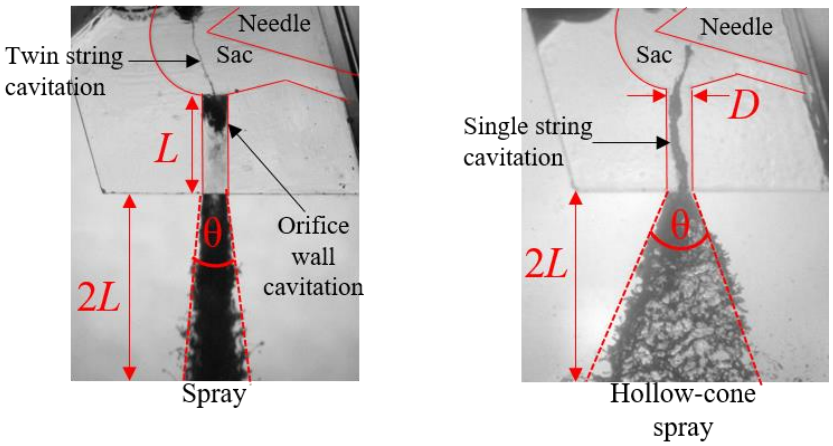

Fig. 3 Definition of spray angle θ

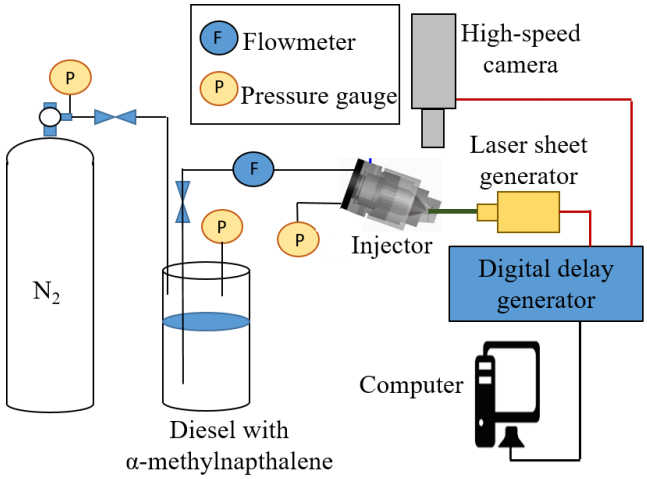

(a) Experimental setup for PIV analysis

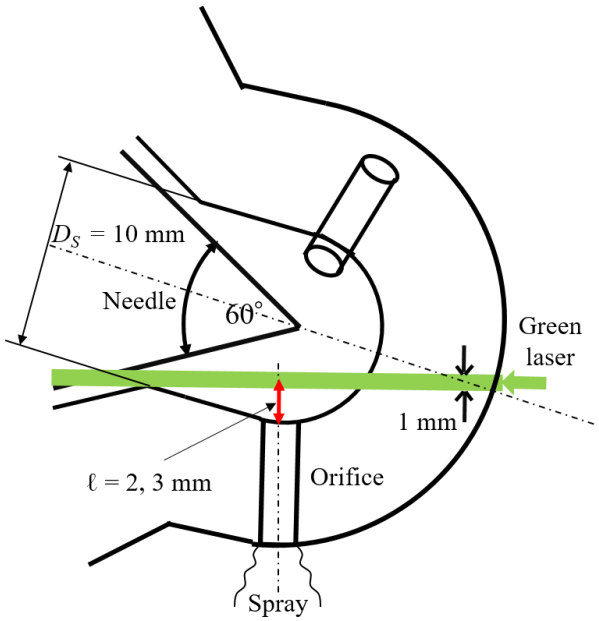

(b) Laser sheet position

Fig. 4 Experimental setup for PIV analysis

[DOI: 10.1299/jfst.2023jfst0023]

4. Results and discussion

4.1 High-speed imaging

Figure 5(a) shows the images of cavitation in the mini-sac injector and liquid jet at Z/D = 1. Hiroyasu et al. (1991) and Sou et al. (2007) have clarified that as mean liquid velocity V in the orifice increases, orifice wall cavitation changes from no cavitation (NC), incipient cavitation (IC), developing cavitation (DC), super cavitation (SP), into hydraulic flip (HF). As shown in Fig. 5(a), at very low mean velocity of V = 11.0 m/s, no cavitation is observed in the orifice and spray angle is narrow (θ = 8°). As V increases to 13.0 m/s, cavitation inception occurs near orifice inlet and spray angle increases to 9 degrees. At higher velocity of V = 14.0 m/s, developing cavitation is formed. For V = 16 m/s, we can observe imperfect hydraulic flip (IHF) and a largely deformed liquid jet (θ = 14°). These results agree well with the previous observations. It should be pointed out that string cavitation (SC) with very small diameter connecting two neighboring orifices are sometimes observed at Z/D = 1. Figure 5(b) shows the bottom view of the sac when SC appears. We clearly observed one or two string cavitations from an orifice to the neighboring orifices. This type of SC was reported by Hayashi et al. (2013) and we will call it twin string cavitation.

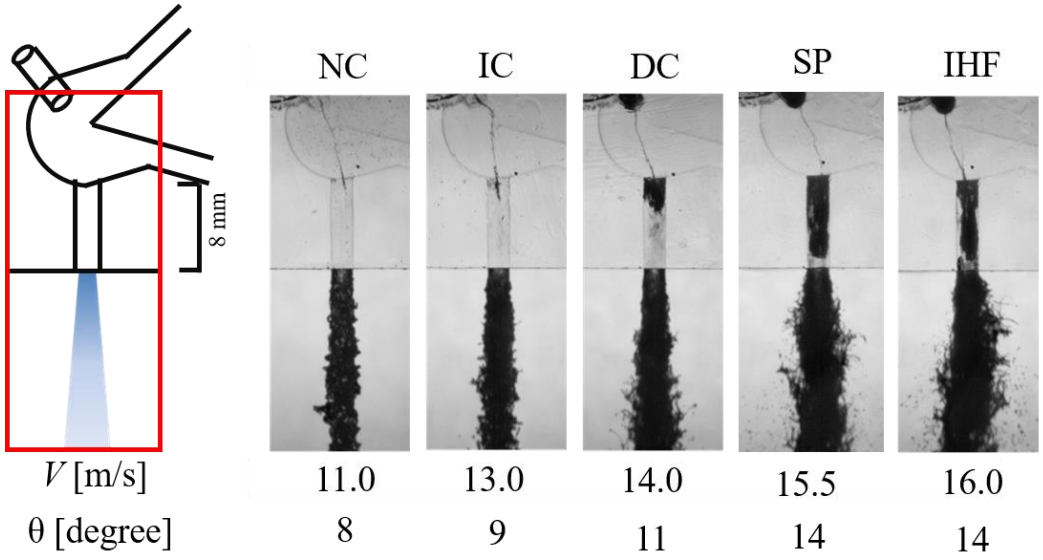

(a) Front view of twin string cavitation, orifice wall cavitation, and liquid jet

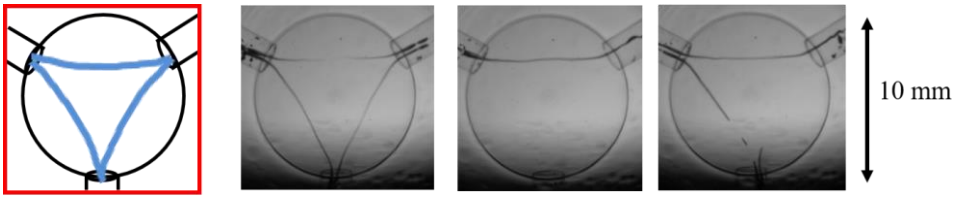

(b) Bottom view of twin string cavitation (V = 13 m/s)

Fig. 5 Images of twin string cavitation and a discharged liquid jet at Z/D = 1

Figure 6 shows the images of cavitation in the injector at very low needle seat gap of Z/D = 0.5. As shown in Fig. 6(a), a string cavitation with large diameter occurs from the needle surface to the orifice exit. Once the string cavitation takes place, it appears steadily to produce a hollow-cone spray with very large spray angle of θ = 43 - 45 degrees. Figure 6(b) shows the bottom view. We can confirm that only one SC appears in two orifices within three orifices due to the odd number of the orifices. This types of SC can be seen in the previous report by He et al. (2016). Since the number and steadiness of the SC is different from that can be observed ad Z/D = 1, we will call it single string cavitation.

Figure 7 shows the probability of SC appearance P_{SC} and spray angle θ. As shown in Fig. 7(a), P_{SC} of single SC is 1 at V > 7 m/s, while P_{SC} of twin SC is about 20%. Measured spray angle is summarized in Fig. 7(b). Spray angle θ at Z/D = 1 and V = 7 - 16 m/s sometimes with twin SC is 5 - 14 degrees, while θ with single SC at Z/D = 0.5 and V = 8 - 15

[DOI: 10.1299/jfst.2023jfst0023]

m/s is almost always about 43 degrees. Hence, we can conclude that twin SC is intermittent and slightly increases spray angle, while single SC is steady and induces very large spray angle.

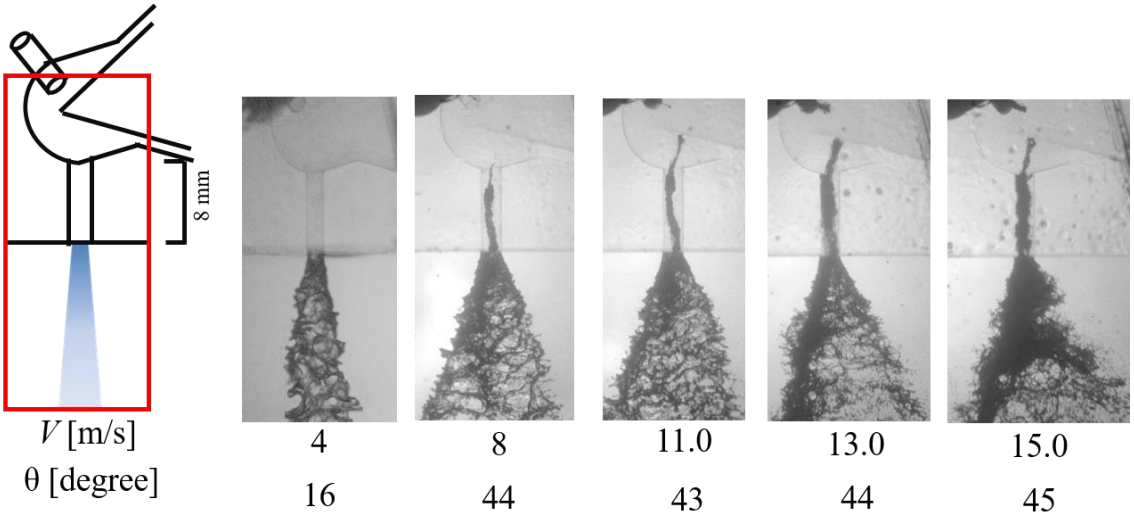

(a) Front view of single string cavitation and a hollow-cone spray

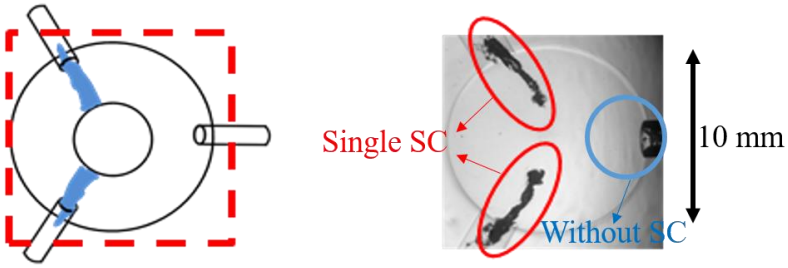

(b) Bottom view of single string cavitation (V = 13 m/s)

Fig. 6 Images of single string cavitation and a discharged liquid jet at Z/D = 0.5

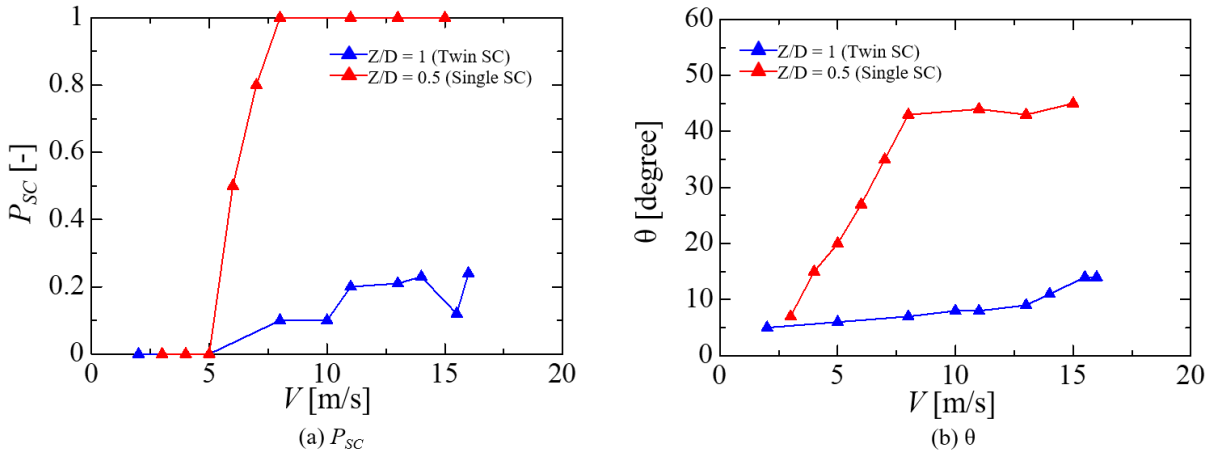

(a) P_{SC} (b) θ

Fig. 7 Probability of string cavitation appearance P_{SC} and spray angle θ

4.2 Velocity distribution by high-speed PIV

This section discusses measured velocity distribution by PIV analysis in the sac upstream of an orifice. Figure 8(a) shows measured velocity distribution with steady single SC at Z/D = 0.5, V = 10.5 m/s and ℓ = 2 mm. We can clearly see the formation of a steady swirling flow in the sac which cannot find by PIV analysis on a plane through the central axis of the sac. It should be noted that the maximum rotational speed is about as large as 70% of axial mean velocity V in the

[DOI: 10.1299/jfst.2023jfst0023]

orifice. As shown in Fig. 8(b), measured circulation Γ in the rectangular section of 6 mm x 3 mm around the orifice is found to be almost constant of Γ = -0.043 m^2/s, which induces the hollow-cone spray by the large centrifugal force.

Figure 9(a) shows velocity and vorticity distributions at Z/D = 0.5, V = 10.5 m/s and ℓ = 2 mm with single SC. We can confirm the large vorticity near the orifice. Figure 9(b) shows the results in the case when there is no single SC due to the odd number of the orifices. We can see a twin swirling flow near the orifice. Based on the above two flow patterns, we illustrate the three-dimensional flow structure in the sac for Z/D = 0.5 with single SC in Fig. 9(c). Since the test injector has three orifices, single SC with strong swirling flow can be formed in only two orifices.

Figure 10 shows calculated Γ in the left half square of 3 mm x 3 mm and that in the right half of 3 mm x 3 mm of the rectangular section of 6 mm x 3 mm. The results at ℓ = 2 mm and 3 mm are almost the same. When twin swirling flow occurs, the magnitude of the circulation Γ in the right half is almost equal to that in the left half, and the sum of two circulations is almost zero. On the other hand, when single swirling flow takes place, the large magnitude of the total circulation induces a hollow-cone spray by the strong centrifugal force.

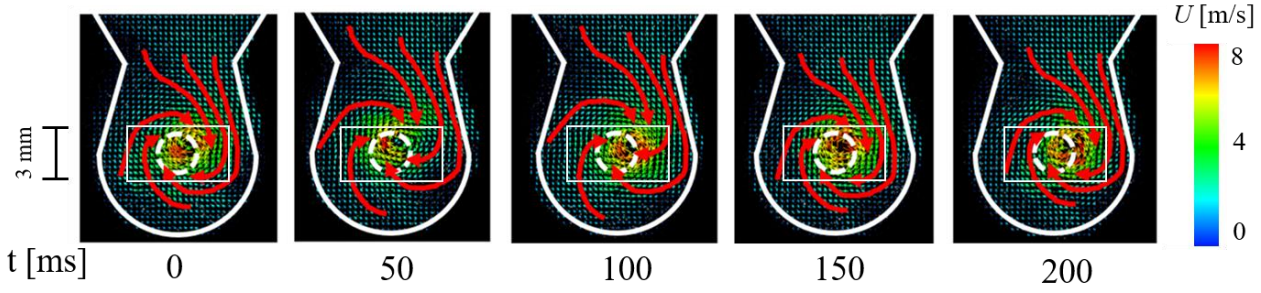

(a) Velocity distribution by high-speed PIV on a plane 2 mm upstream of an orifice with single SC

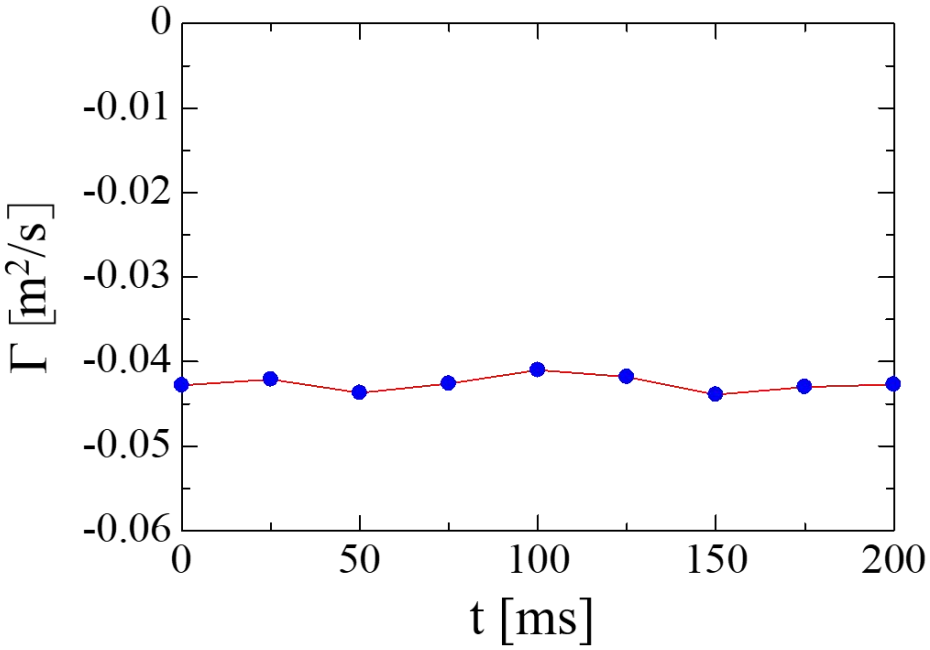

(b) Measured circulation Γ in the region of 6 mm x 3 mm near the orifice

Fig. 8 Measured velocity distribution and circulation at Z/D = 0.5, V = 10.5 m/s and ℓ = 2 mm

[DOI: 10.1299/jfst.2023jfst0023]

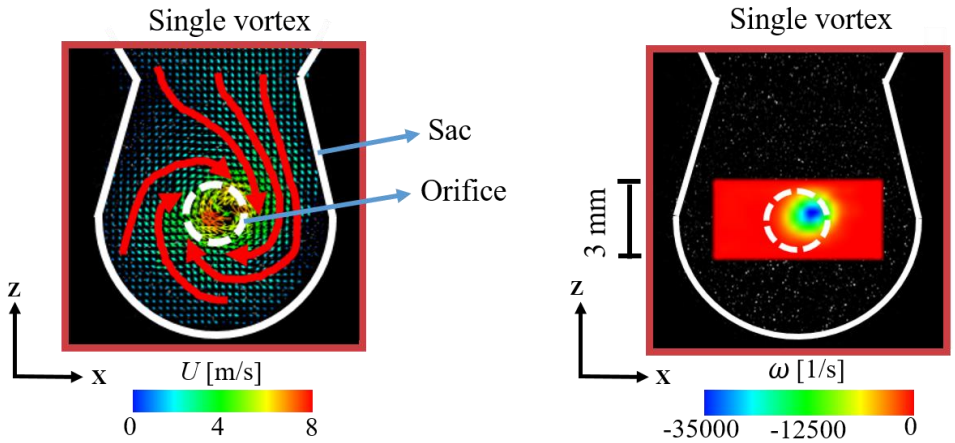

(a) Upstream of an orifice with single vortex

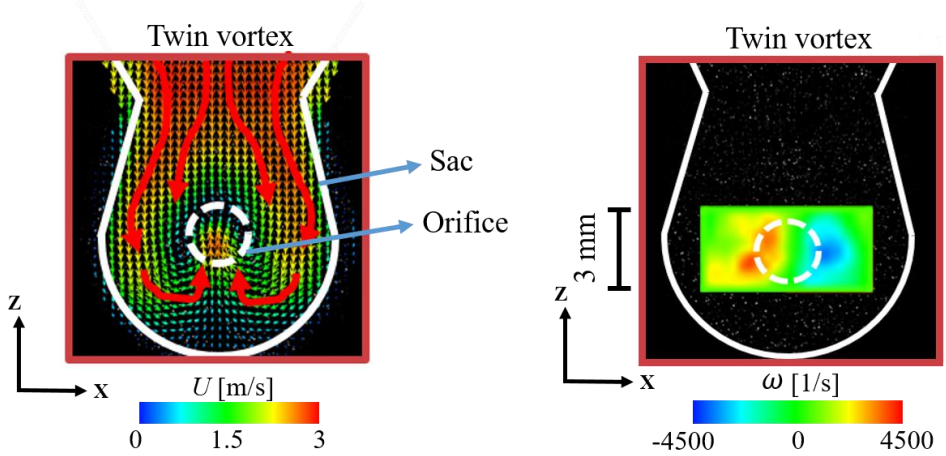

(b) Upstream of an orifice with twin vortex

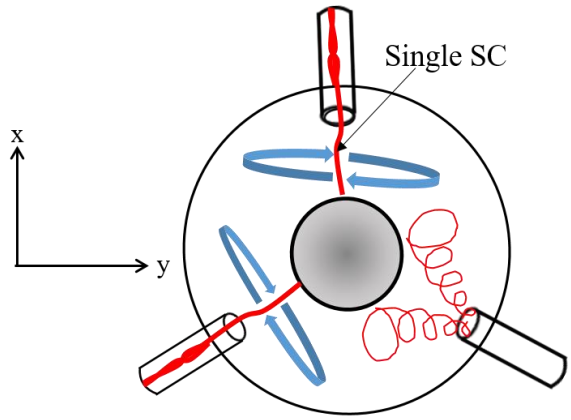

(c) Flow pattern in the sac at $Z/D = 0.5$

Fig. 9 Velocity distribution and vorticity in the sac at $Z/D = 0.5$, $V = 10.5$ m/s and $\ell = 2$ mm

[DOI: 10.1299/jfst.2023jfst0023]

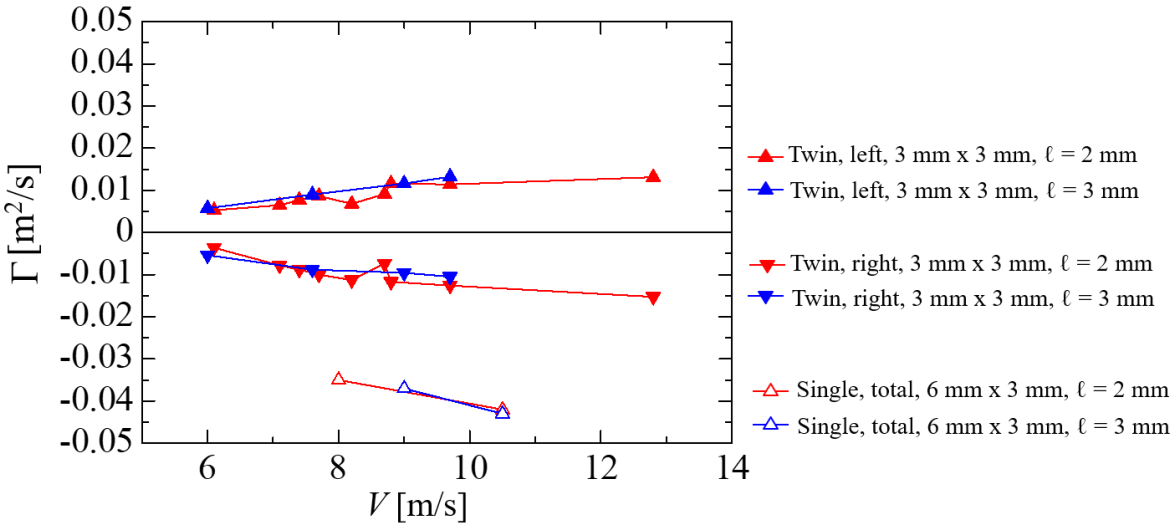

Fig. 10 Measured circulation in the sac at $Z/D = 0.5$

5. Conclusions

In order to investigate string cavitation flow in a diesel fuel injector, we carry out visualization of string cavitation in a transparent injector at different needle seat gaps as well as PIV analysis in the planes perpendicular to the axis of an orifice. As a result, it was found that twin string cavitation with small diameter appears intermittently at low needle seat gap of $Z/D = 1$ due to the formation of the twin swirling flow upstream of an orifice. In contrast, at the very low needle lift of $Z/D = 0.5$, stable single string cavitation with larger diameter is induced by the steady single swirling flow upstream of an orifice, which induces a steady spiral flow in the orifice and a hollow-cone spray, and significantly increases spray angle.

Acknowledgements

The authors would like to express their deepest gratitudes to Mr. Katsuhisa Nakamichi, Mr. Masashi Wakisaka, Mr. Taro Bando, Ms. Okami Natsuha, Mr. Dongping Shen and Mr. Yoshiyuki Matsubara for their assistances.

References

Bergwerk, W., Flow Pattern in Diesel Nozzle Spray Holes, Proceedings of the Institution of Mechanical Engineers, Vol. 173, No.1 (1959), pp. 655–660, DOI:10.1243/PIME_PROC_1959_173_054_02.

Duke, D. J., Matusik, K. E., Kastengren, A. L., Swantek, A. B., Sovis, N., Payri., R., Viera, j. P., and Powell, C. F., X-Ray Radiography of Cavitation in a Beryllium Alloy Nozzle, International Journal of Engine Research, Vol. 18, No. 1-2 (2017), pp. 35-50, DOI:10.1177/1468087416685965.

Gavaises, M., Andriotis, A., Papoulias, D., Mitroglou, N., and Theodorakakos, A., Characterization of String Cavitation in Large-Scale Diesel Nozzles with Tapered Holes, Physics of Fluids, Vol. 21, No. 5 (2009), DOI: 10.1063/1.3140940.

Guan, W., He, Z., Duan, L., Cao, T., Sun, S., and Zhang, L., Optical Investigations of Nozzle Geometrical and Dynamic Factors on Formation and Development Characteristics of String Cavitation with Large-Scale Diesel Tapered-Hole Nozzle, International Journal of Engine Research, Vol. 22 (2021), pp. 3147-3163, DOI: 10.1177/1468087420969332.

Hayashi, T., Suzuki, M., and Ikemoto, M., Effects of Internal Flow in a Diesel Nozzle on Spray Combustion, International Journal of Engine Research, Vol 14, No. 6 (2013), pp 646-654, DOI: 10.1177/1468087413494910.

He, Z., Zhang, Z., Guo, G., Wang, Q., Leng, X., and Sun, S., Visual Experiment of Transient Cavitating Flow

Characteristics in the Real-Size Diesel Injector Nozzle, International Communication in Heat and Mass Transfer, Vol 78 (2016), pp 13-20, DOI: 10.1016/j.icheatmasstransfer.2016.08.004.

Hiroyasu, H., Arai, M., and Shimizu, M., Break-up Length of a Liquid Jet and Internal Flow in a Nozzle, Proceedings of the 5th International Conference on Liquid Atomization and Spray Systems (1991), pp. 275–282.

Miranda, R., Chaves, H., and Obermeier, F., Imaging of Cavitation, Hollow Jets and Jet Branching at Low Lift in a Real Size VCO Nozzle, in Proc. Of ILASS-Europe 2002, 18th Annual Conf. On Liquid Atomization and Spray Systems (2002).

Mitroglou, N., Gavaises, M., Nouri, J.M., and Arcoumanis, C., Cavitation Inside Enlarged and Real-Size Fully Transparent Injector Nozzles and Its Effect on Near Nozzle Spray Formation, In DIPSI Workshop 2011 on Droplet Phenomena and Spray Investigation (2011).

Pratama, R. H., Sou, A., Katsui, T., and Nishio, S., String Cavitation in a Fuel Injector, Atomization and Spray, Vol 27, No. 3 (2017), pp 189-205, DOI: 10.1615/AtomizSpr.2016016276.

Prasetya, R., Sou, A., Oki, J., Nakashima, A., Nishida, K., Wada, Y., Ueki, Y., and Yokohata, H., Three-Dimensional Flow Structure and String Cavitation in a Fuel Injector and Their Effects on Discharged Liquid Jet, International Journal of Engine Research, Vol. 22 (2021), pp. 243-256, DOI: 10.1177/1468087419835697.

Schmidt, D. P., and Corradini, M. L., The Internal Flow of Diesel Fuel Injector Nozzles: A Review, International Journal of Engine Research, Vol 14, No .2 (2001), pp. 1-22, DOI: 10.1243/1468087011545316.

Soteriou, C., Andrews, R., and Smith, M., Direct Injection Diesel Sprays and the Effect of Cavitation and Hydraulic Flip on Atomization. In SAE Technical Papers (1995), pp. 27–52, DOI: 10.4271/950080.

Sou, A., Hosokawa, S. and Tomiyama, A., Effects of Cavitation in a Nozzle on Liquid Jet Atomization, International Journal of Heat and Mass Transfer, Vol. 50, No. 17–18 (2007), pp. 3575–3582, DOI: 10.1016/j.ijheatmasstransfer.2006.12.033.

Sou, A., Maulana, M.I., Isozaki, K., Hosokawa, S. and Tomiyama, A., Effects of Nozzle Geometry on Cavitation in Nozzles of Pressure Atomizers, Journal of Fluid Science and Technology, Vol. 3, No. 5 (2008a), pp. 622–632, DOI: 10.1299/jfst.3.622.

Sou, A., Maulana, M.I., Hosokawa, S. and Tomiyama, A., Ligament Formation Induced by Cavitation in a Cylindrical Nozzle. Journal of Fluid Science and Technology, Vol. 3, No. 5 (2008b), pp. 633–644, DOI: 10.1299/jfst.3.633.

Wei, Y., Zhang, H., Fan, l., Gu, Y., Leng, X., Deng, Y., and He, Z., Experimental Study into the Effects of Stability Between Multiple Injections on the Internal Flow and Near Field Spray Dynamics of a Diesel Nozzle, Energy, Vol. 248 (2022), DOI: 10.1016/j.energy.2022.123490.

[DOI: 10.1299/jfst.2023jfst0023]